Hindawi Publishing Corporation
Indian Journal of Materials Science
Volume 2015, Article ID 690568, 9 pages
http://dx.doi.org/10.1155/2015/690568

Research Article

Synthesis, Characterization, and Investigation of Visible Light Photocatalytic Activity of C Doped TiO_2/CdS Core-Shell Nanocomposite

Atul B. Lavand,[1] Yuvraj S. Malghe,[1] and Suraj H. Singh[2]

[1]*Department of Chemistry, The Institute of Science, 15 Madam Cama Road, Mumbai 400032, India*
[2]*Department of Energy Science & Engineering, Indian Institute of Technology, Mumbai 400076, India*

Correspondence should be addressed to Yuvraj S. Malghe; ymalghe@yahoo.com

Received 15 May 2015; Accepted 7 September 2015

Academic Editor: Ana Cremades

Carbon (C) doped TiO_2/CdS core-shell nanocomposite (C/TiO_2/CdS) was synthesized using microemulsion method. Synthesized powder was characterized using X-ray diffraction (XRD), Fourier transform infrared spectroscopy (FTIR), energy dispersive X-ray spectroscopy (EDX), transmission electron microscopy (TEM), and UV-visible spectrophotometery. TEM images reveal that C/TiO_2/CdS core-shell heterostructure is successfully prepared with CdS as a core and C doped TiO_2 as a shell. UV-visible absorption spectra show that CdS nanoparticles act as a sensitizer and effectively enhance the photoabsorption capacity of C/TiO_2/CdS nanocomposite in visible region. Visible light photocatalytic activity of synthesized nanocomposite was evaluated for the degradation of methylene blue. C/TiO_2/CdS core-shell nanocomposite exhibits better photocatalytic activity as compared to bare TiO_2, CdS, CdS/TiO_2, and C doped TiO_2.

1. Introduction

Photocatalysis can be used as an abundant and clean energy source for different purposes like environmental remediation, clean energy production, and so forth [1–3]. Recent day's lot of research is going on, to develop novel photocatalyst and improve its efficiency in visible/solar light [4–6]. In photocatalysis, light of energy greater than the semiconductor band gap which excites electron from valence band to conduction band is required. Among various photocatalysts reported TiO_2 has attracted special attention due to its unique physical and chemical properties such as strong oxidizing and reducing ability, good permeability, better optical properties, chemical stability, low cost, and corrosion resistance [7–9]. Among the various forms of TiO_2, anatase TiO_2 exhibits better photocatalytic activity [10]. It has the band gap 3.2 eV and requires UV light ($\lambda \leq 387$ nm) to activate. Solar spectrum consists of 5% UV and ~45 to 50% visible light. To utilize visible light portion it is necessary to modify TiO_2. One of the ways to modify TiO_2 is to couple it with semiconductor with narrow band gap. CdS with band gap 2.4 eV is considered as one of the ideal sensitizers due to unique position of its conduction and valence band edges [11–14]. Unfortunately CdS/TiO_2 composite suffers from major disadvantage that is quick recombination of photogenerated charge carriers which decreases the photocatalytic performance. To compensate this problem it is necessary to modify this composite by doping it with metals or nonmetals. Few reports are available in literature [13, 15, 16] regarding the preparation of hybrid materials in which Pt or C nanotubes are incorporated. These materials act as an excellent electron acceptor/transporter centre and effectively facilitate the migration of photoinduced electrons and suppress the charge combination in electron-transfer process due to electronic interaction between them and CdS/TiO_2 composite. This effectively increases the photocatalytic activity. Carbonaceous materials are very popular in photocatalysis due to their wide range visible light absorption capacity and better adsorption power of organic pollutants [17, 18]. In such hybrid materials strong synergetic effect can be achieved. Therefore, in a present work we have synthesized C doped TiO_2/CdS nanocomposite using microemulsion method and

its visible light photocatalytic activity was investigated for the degradation of methylene blue dye.

2. Materials and Methods

2.1. Materials. Methylene blue (MB) practical grade was obtained from Hi Media Laboratories, Mumbai, and used without any further purification. Titanium isopropoxide $Ti(iOPr)_4$ was purchased from Sigma Aldrich, Mumbai, and used as a source of titanium. All these chemicals, cyclohexane, n-butanol, N,N,N-cetyl trimethyl ammonium bromide (CTAB), acetone, cadmium nitrate ($Cd(NO_3)_2{\cdot}4H_2O$), sodium sulphide flakes (Na_2S), sodium hydroxide (NaOH), and ethanol (99.7%), used for synthesis are of AR grade and are procured from SD Fine Chemicals, Mumbai, India, and are used without further purification.

2.2. Synthesis of Photocatalyst

2.2.1. Synthesis of CdS Nanoparticles. 50 mL 1 M cadmium nitrate, 25 mL double distilled water, 25 mL ethanol, and 0.01 M CTAB were mixed in a beaker and stirred for 30 min continuously. 50 mL 1 M Na_2S, 25 mL ethanol, and 25 mL double distilled water were added to the above solution and stirred for 30 min. To this mixture 20 mL 2 M NaOH was added dropwise with continuous stirring. It gives light yellow precipitate. Mixture thus formed was transferred to autoclave (with Teflon-inner-liner) and kept in an oven at 100°C for 2 h. Later it was cooled to the room temperature and the residue obtained was separated using centrifugation, washed several times with distilled water followed by ethanol and finally with acetone, and dried at 40°C to get pure CdS.

2.2.2. Synthesis of Pure and C Doped TiO_2 Nanoparticles. Pure and C doped TiO_2 nanoparticles were prepared using microemulsion method reported in our previous work [19]. 60 mL cyclohexane, 15 mL n-butanol, and 6 g CTAB were mixed together and mixture was stirred for 15 min. To this microemulsion solution containing 3 mL water and 9 mL 1 M titanium isopropoxide was added dropwise with constant stirring. This mixture was transferred to autoclave (with Teflon-inner-liner) and kept in an oven at 150°C for 2 h. Later it was cooled to the room temperature and the residue obtained was separated by centrifugation, washed several times with distilled water followed by ethanol and finally with acetone, and dried at 40°C. The product obtained was used as a precursor. This precursor was calcined in furnace at 300 and 500°C to get C doped and pure TiO_2, respectively.

2.2.3. Synthesis of C Doped TiO_2/CdS Core-Shell Nanocomposite (C/TiO_2/CdS). 80 mL cyclohexane, 20 mL butanol, 4.0 g CTAB, and 6 mL 1 M cadmium nitrate were mixed in a beaker and stirred for 30 min. To this microemulsion 6 mL 1 M Na_2S was added and mixture was stirred for 30 min. Afterwards, 6 mL 1 M titanium isopropoxide was added dropwise with constant stirring. This mixture was transferred to autoclave (with Teflon-inner-liner) and kept in an oven at 150°C for 2 h. Later it was cooled to the room temperature and the residue obtained was separated using centrifugation, washed several times with distilled water followed by ethanol and finally with acetone, and dried at 40°C. Dried powder was calcined at 300 and 500°C for 2 h to get C doped and pure TiO_2/CdS nanocomposite.

2.3. Characterizations. X-ray diffraction (XRD) patterns of all the calcined powders were recorded using Rigaku, (Model-Miniflex II) X-ray diffractometer with Cu Kα radiation ($\lambda = 0.15418$ nm) at a scan rate $2^\circ\,\text{min}^{-1}$. Average particle sizes were calculated using Debye-Scherrer equation $t = n\lambda/B\cos\theta$, where t is average particle size, $n = 0.9$, and B is full width of line at half of the maximum intensity (FWHM). FTIR spectra of samples were recorded with FTIR spectrophotometer (Bruker). Qualitative elemental analysis of the calcined powders was carried out using energy dispersive X-ray spectroscopy (EDX) using JEOL-JSM instruments. Particle size of the compounds prepared in this work was studied using transmission electron microscope (TEM) (FEI, USA, Model-Technai-G^2). UV-visible spectrophotometer (Shimadzu, Model-1800) was used to study the band gap energy of synthesized nanopowders.

2.4. Photocatalytic Activity Study. Visible light photocatalytic activities of synthesized catalysts were evaluated for the degradation of methylene blue (MB) using 65 W compact fluorescent lamp ($\lambda > 420$ nm, Philips, Mumbai). Photodegradation was carried out using a homemade photo reactor with water jacket to maintain temperature through experiment. Distance between the light and the reaction vessel is fixed at 10 cm. 0.05 g photocatalyst powder was dispersed in 50 mL 10 ppm MB solution. Prior to photocatalytic measurements, the aqueous suspension was stirred in the dark for 30 min to attain adsorption-desorption equilibrium. After reaction suspension was irradiated with visible light. At specific time intervals, 5 mL aliquot was taken out, catalyst was separated using centrifugation, and concentration of MB in the supernatant solution was estimated from UV-visible spectra recorded in the wavelength range 200–800 nm.

3. Results and Discussion

3.1. X-Ray Diffraction (XRD) Study. XRD patterns of C doped TiO_2, CdS, and C doped TiO_2/CdS core-shell nanoparticles were recorded and are presented in Figure 1. XRD pattern of CdS shows peaks which correspond to crystal planes (111), (200), (220), (311), (400), and (420) and are in good agreement with pure cubic CdS phase (JCPDS card number: 65-2887). Broadness of the peaks suggests that CdS particles are very small. XRD pattern of TiO_2 precursor calcined at 300°C (C doped TiO_2) suggests that at this temperature TiO_2 formed is having anatase phase. Peaks at 2θ equal to 25.26, 38.16, 48.17, 54.03, 64.69, 68.16, 71.10, and 76.4° are assigned for (101), (004), (200), (105), (211), (204), (110), (220), and (215) *hkl* planes and are in good agreement with JCPD data file number 841285 (lattice planes of anatase TiO_2 phase). XRD pattern of C/TiO_2/CdS core-shell nanocomposite suggests that this composite formed is a mixture of cubic CdS

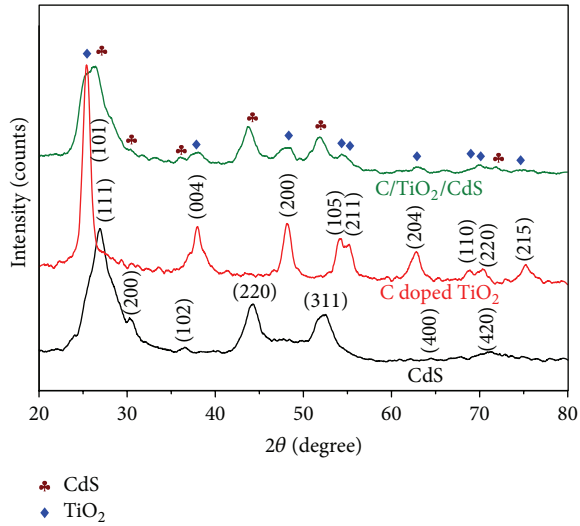

Figure 1: XRD patterns of CdS, C doped TiO_2, and C/TiO_2/CdS nanocomposite.

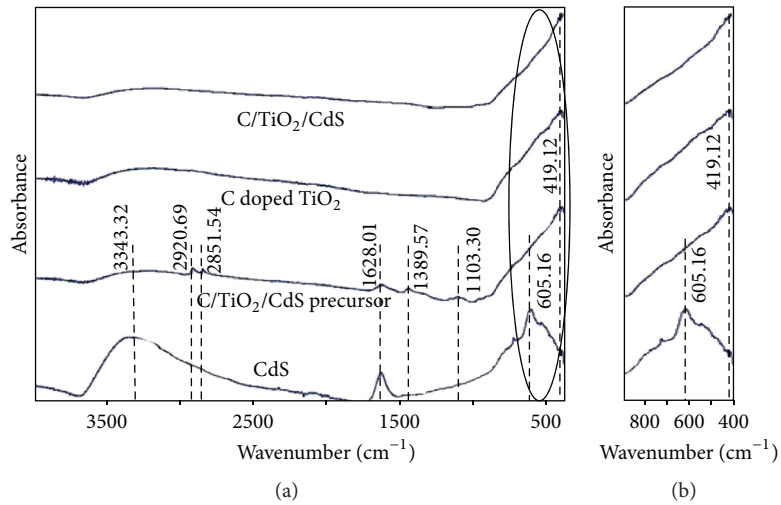

Figure 2: FTIR spectra of CdS, C/TiO_2/CdS precursor, C doped TiO_2, and C/TiO_2/CdS nanocomposite; (b) expanded view of FTIR spectra.

and anatase TiO_2 phase. Average crystallite sizes of all the compounds were calculated using Debye-Scherer equation and data is presented in Table 1.

3.2. FTIR Study. FTIR spectra of CdS, C/TiO_2/CdS precursor, C doped TiO_2, and C/TiO_2/CdS nanocomposite are shown in Figure 2. Precursor samples show bands at 3000–3500 cm^{-1} attributed to stretching vibration modes of OH group (TiO_2-OH) (Figure 2(a)). It was believed that such TiO_2-OH groups arise due to the hydrolysis reaction in the microemulsion process [20]. Peak at 1628 cm^{-1} is attributed to bending modes of –OH groups of water molecules adsorbed on the surface of catalyst [21]. Peak at 1389 cm^{-1} can be assigned to C-O stretching in carbonyl. Peak at 2920 cm^{-1} is assigned as characteristic peak of ammonium. Peak at 2851 cm^{-1} is due to symmetrical stretching vibration of methyl group. This information indicates that –OH and –C=O functional groups are present in precursor. Figure 2(b) shows that C doped TiO_2 and C/TiO_2/CdS samples show a band corresponding to Ti-O-Ti vibration at about 419 cm^{-1}. Pure CdS shows a band at 605 cm^{-1} ascribed to Cd-S stretching [22, 23]. C/TiO_2/CdS sample does not show peak which corresponds to Cd-S stretching at 605 cm^{-1} which might be due to formation of core-shell structure with CdS as core and C doped TiO_2 as shell. FTIR spectra of product obtained after heating the precursor at 300°C for 2 h show no absorption peak in higher frequency region but give the sharp peak below 500 cm^{-1} which may be due to stretching frequency of Ti-O-Ti bond in titanium dioxide.

3.3. Energy Dispersive X-Ray Spectroscopy (EDX) Study. Figure 3 represents EDX spectra of (a) C doped TiO_2, (b) CdS, and (c) C/TiO_2/CdS core-shell nanocomposite. EDX analysis shows that CdS nanoparticles contain only Cd and S elements with 60.83 and 39.17 at%, respectively. TiO_2 precursor calcined at 300°C contains C, Ti, and O with

Table 1: Characteristic properties of photocatalyst.

Sample	Particle size/nm[a]	C/at%[b]	Band gap (E_g)/eV[c]	Reaction parameters	
				Rate constant (k)/min^{-1}	R^2
Pure TiO_2	16.2	—	3.14	0.0045	0.949
C doped TiO_2	11.3	13.41	2.86	0.0108	0.995
CdS	6.2	—	1.82	0.0053	0.952
C/TiO_2/CdS core-shell	10.5	14.62	2.28	0.0326	0.958

a: particle sizes were obtained from TEM images.
b: C content was obtained from EDX spectra.
c: λ values were obtained from onset of light absorption edges and E_g values were calculated using Tauc plots.

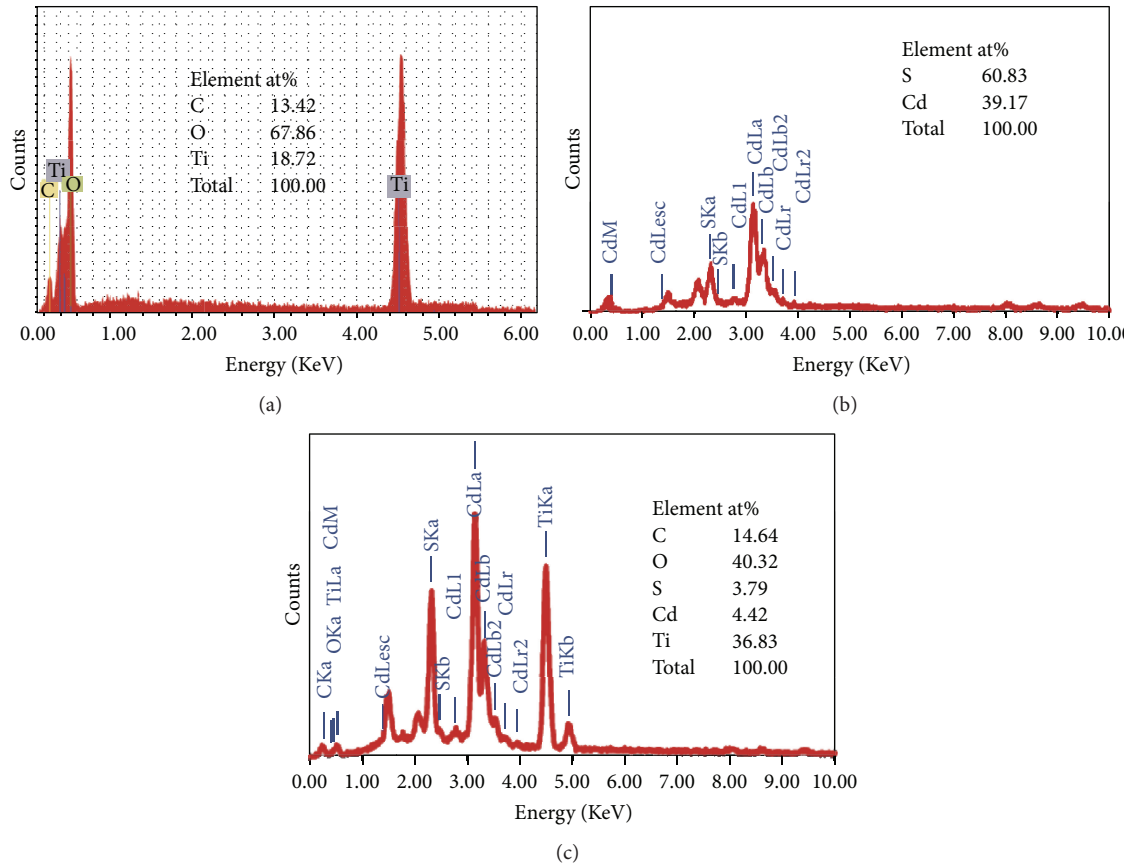

Figure 3: EDX spectra of (a) C doped TiO_2, (b) CdS, and (c) C/TiO_2/CdS.

13.42, 18.72, and 67.86 at%, respectively. EDX analysis clearly showed the presence of Cd, S, C, Ti, and O elements in the composite sample with 4.42, 3.79, 14.64, 36.83, and 40.32 at%, respectively.

3.4. Transmission Electron Microscopy (TEM) Study. TEM image of C doped TiO_2 is presented in Figure 4(a). This image shows that C doped TiO_2 particles are spherical in shape and average particle size was found to be 10 to 12 nm. TEM image of CdS nanoparticle is shown in Figure 4(b). This image shows that CdS nanoparticles are spherical in shape and well dispersed. Average particle size is varying between 6 and 7 nm. Figure 4(c) represents the TEM image of C/TiO_2/CdS core-shell nanocomposite. From this figure we can see that CdS particles act as a core and C doped TiO_2 as a shell. A selected area electron diffraction (SAED) pattern of all the samples (inset) shows distinct rings indicating their crystalline nature.

C/TiO_2/CdS core-shell nanospheres were prepared by the microemulsion method. First Cd^{2+} ions from the aqueous $Cd(NO_3)_2$ solution form $Cd(OH)_2$ microemulsion. Addition of sulfur in this solution gives CdS nanospheres by substituting OH^- ions with S^{2-} ions. After the addition of TTIP, $Ti(OH)_4$ layer gets formed on CdS. This precursor was heated at 300°C for 2 h yielding C/TiO_2/CdS core-shell nanocomposite. The possible mechanism of the formation of C/TiO_2/CdS core-shell nanocomposite is described schematically in Figure 5.

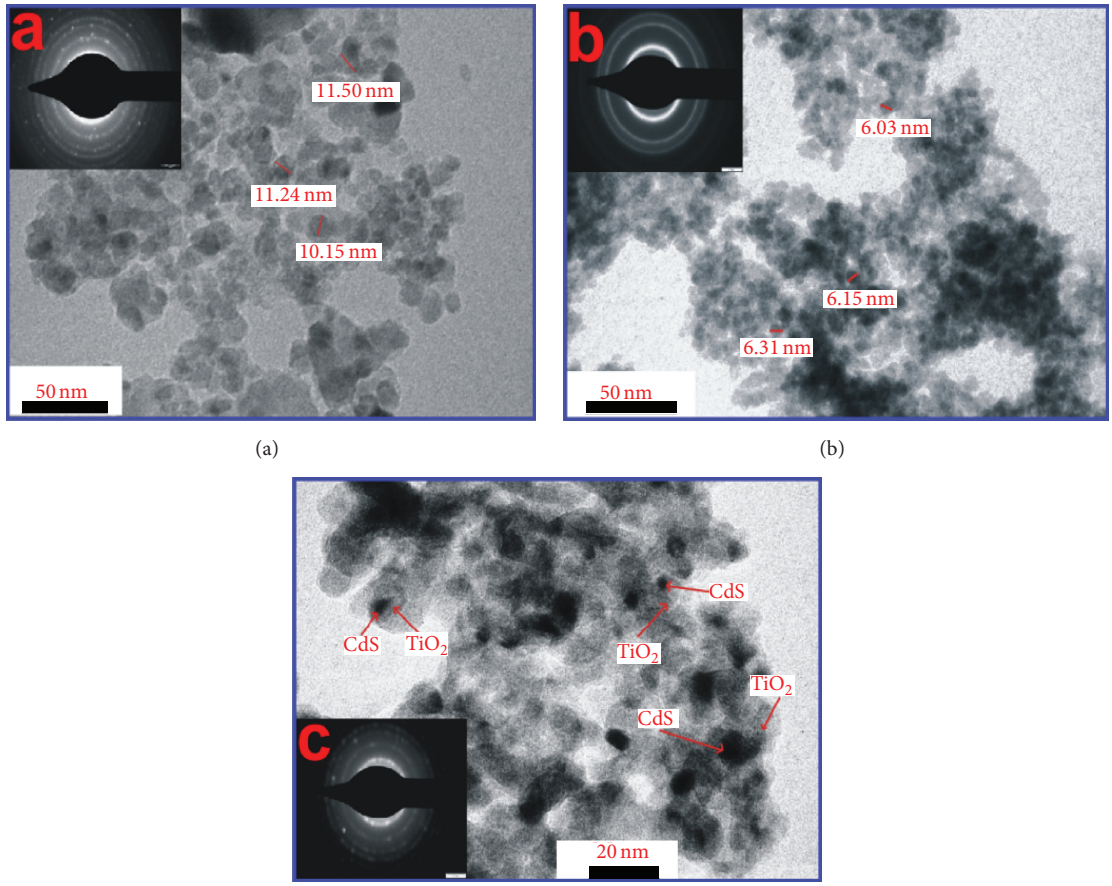

Figure 4: TEM images of (a) C doped TiO_2, (b) CdS, and (c) C/TiO_2/CdS core-shell nanocomposites.

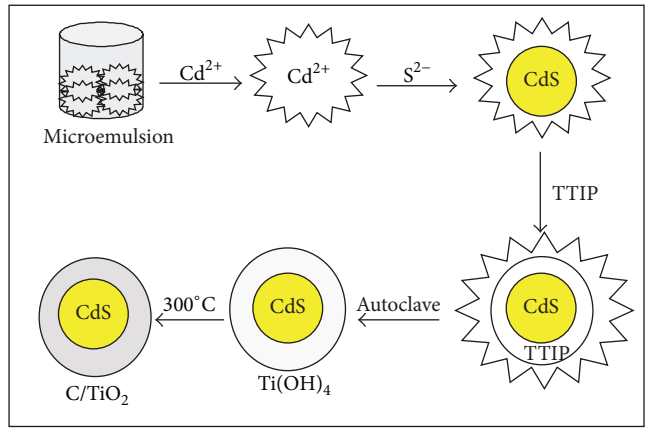

Figure 5: Schematic diagram showing the steps of formation of C/TiO_2/CdS core/shell nanospheres by a microemulsion method.

3.5. UV-Visible Spectrophotometery Study. Photo response of pure CdS, C doped TiO_2, and C/TiO_2/CdS was studied from their UV-visible absorption spectra and presented in Figure 6. Pure TiO_2 sample obtained at 500°C is white color and exhibits fundamental absorption edge at 387 nm. C doped TiO_2 prepared at 300°C is blackish in color and shows absorption peak in visible region with band edge located at 433 nm. It indicates that C doping enhances absorption power and shifts absorption edge from UV to visible region. CdS nanopowder is yellow color and shows absorption edge around 680 nm. C/TiO_2/CdS core-shell nanopowder obtained at 300°C is light grayish yellow color and shows absorption edge near 600 nm, indicating the effective enhancement in photoabsorption capacity in visible

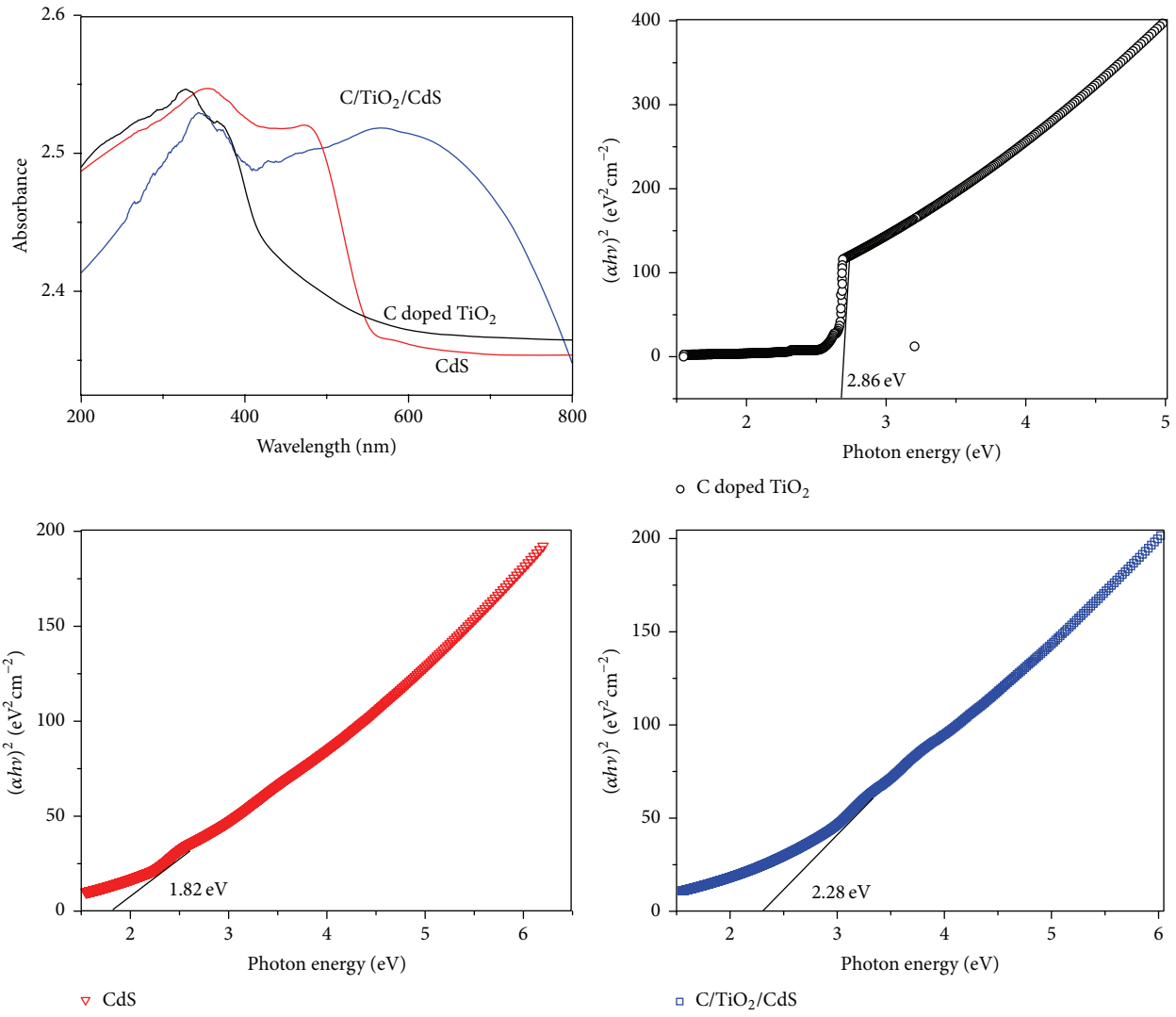

FIGURE 6: UV-visible absorption spectra and Tauc plots of pure CdS, C doped TiO_2, and C/TiO_2/CdS core-shell nanoparticles.

region. Optical band gap (E_g) was determined using Tauc equation, $\alpha h\nu = A(h\nu - E_g)n/2$, where α is absorption coefficient, ν is light frequency, A is proportionality constant, and E_g is band gap. Band gaps of CdS, C doped TiO_2, and C/TiO_2/CdS nanocomposite estimated from Tauc plots (Figure 6) are 1.82, 2.86, and 2.28 eV, respectively. This suggests that nanosized CdS works as a sensitizer and effectively increases the visible light absorption capacity of C doped TiO_2.

3.6. Visible-Light Photocatalytic Activity Study. UV-visible spectra of MB solution irradiated with visible light in presence of C/TiO_2/CdS core-shell nanopowder at different time intervals were recorded and are presented in Figure 7. These spectra show that peak intensity at 688 nm decreases as the irradiation time increases. This is may be due to degradation of MB. Decrease in the concentration of MB was monitored by examining the variation in UV-visible spectra at 688 nm. Degradation of MB as a function of irradiation time in presence of different catalysts is presented in Figure 8(a). It

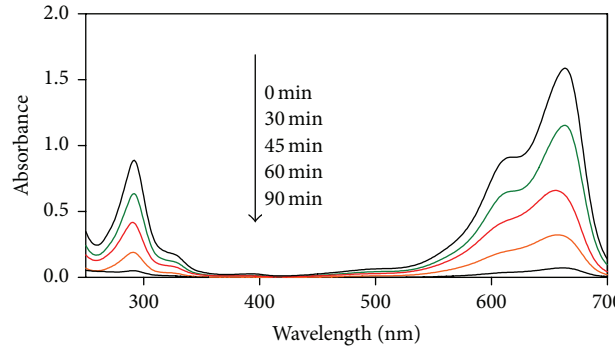

FIGURE 7: UV-visible absorption spectra of MB aqueous solution irradiated with visible light at different time intervals in presence of C/TiO_2/CdS nanocomposite.

shows that in absence of catalyst (i.e., photolysis process) MB dye is quite stable. In presence of C/TiO_2/CdS core-shell nanocomposite ~97% of MB was degraded within

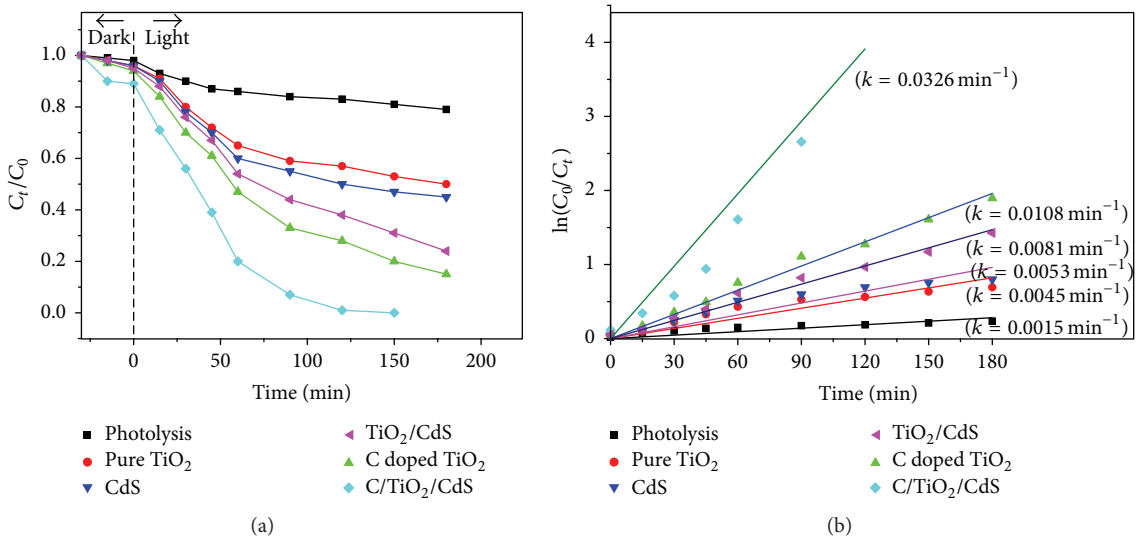

FIGURE 8: (a) Visible light photocatalytic degradation of MB in presence of pure TiO_2, C doped TiO_2, CdS, C/TiO_2/CdS, and TiO_2/CdS. (b) Plot of $\ln(C_0/C_t)$ against reaction time for different photocatalyst.

90 min. Kinetics of MB degradation in visible light was also studied. Graph of $\ln(C_0/C)$ against reaction time shows linear relationship, which indicates that photodegradation of MB follows first-order kinetics (Figure 8(b)). Rate constants (K) and R^2 values for corresponding reactions were calculated and are presented in Table 1. The order of rate constants in presence of different catalyst is C/TiO_2/CdS > C doped TiO_2 > CdS > pure TiO_2. It is in good agreement with the results obtained from photocatalytic degradation curves. C/TiO_2/CdS core-shell nanocomposite shows higher photocatalytic activity as compared to pure CdS, pure TiO_2, and C doped TiO_2. It may be attributed to small size of catalyst and increase in its photoabsorption strength by lowering the band gap energy. Reusability of C/TiO_2/CdS core-shell nanocomposite was tested by reusing the recovered photocatalyst for multiple cycles and results obtained are presented in Figure 9. This figure shows that photocatalytic activity of catalyst does not change significantly up to third cycle indicating that the catalyst is quite stable and can be reused.

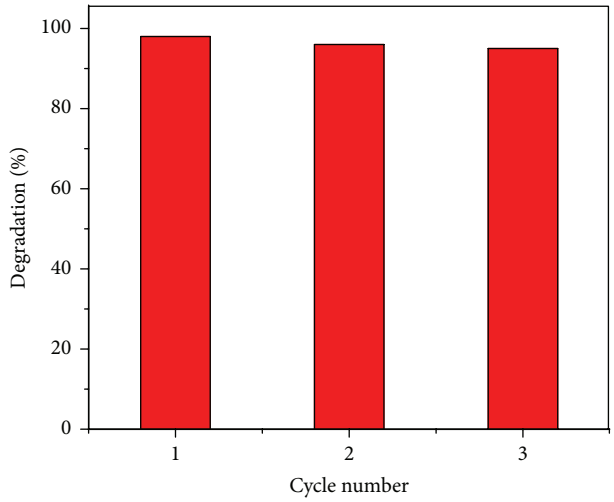

FIGURE 9: Reuse of photocatalyst.

3.7. Degradation Mechanism. Photocatalytic degradation of MB dye can be attributed to the chemical reactions of active species like $OH^\bullet$ and $O_2^{\bullet-}$ with dye molecules on the surface of photocatalyst [24]. The enhancement of photocatalytic activity of C/TiO_2/CdS core-shell nanocomposite heterostructure is due to effective coupling of CdS and C doped TiO_2 as shown in Figure 10. Interstitial C doping can create intraband gap state close to the valence band edge of TiO_2. Thus C doping leads to the narrowing of the band gap in TiO_2 which increases its photoabsorption capacity in visible region. When C/TiO_2/CdS nanocomposite is exposed to visible light, photogenerated electrons are injected from conduction band of CdS to the conduction band of TiO_2, producing high concentration of electrons in the conduction band of TiO_2. On the other hand, holes generated on CdS remain on the valence band of CdS which gives effective charge separation of electron and holes [25]. Meanwhile, the C species could trap the part of photogenerated holes, which potentially reacts with the water adsorbed on the surface of photocatalyst and forms reactive hydroxyl radicals ($OH^\bullet$). Conduction band electrons accumulated on the surface of TiO_2 react with dissolved oxygen in water and produce highly oxidative species such as superoxide radical ($O_2^\bullet$). These highly reactive radicals ($OH^\bullet$ and $O_2^\bullet$) subsequently decompose organic substrate (MB) into CO_2 and H_2O.

4. Conclusions

C/TiO_2/CdS core-shell nanocomposites have been successfully synthesized using microemulsion method. C/TiO_2/CdS nanocomposite shows red shift in the absorption spectra

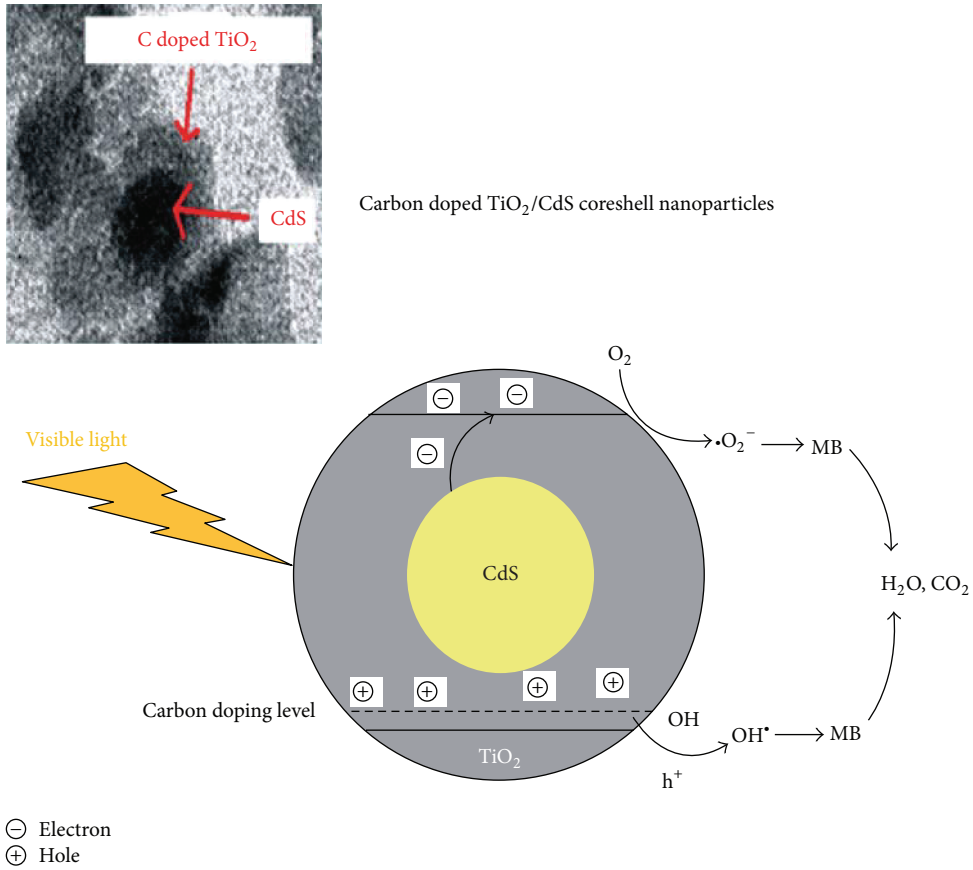

Figure 10: Photoinduced electron-hole pair formation mechanism at C/TiO_2/CdS core-shell nanocomposite surface.

attributed to enhancement in the photoabsorption capacity. C/TiO_2/CdS nanocomposite prepared in the present work exhibits better visible light photocatalytic activity compared to other photocatalysts for MB degradation. Photocatalyst prepared is stable and reusable.

Conflict of Interests

The authors declare that there is no conflict of interests regarding the publication of this paper.

Acknowledgments

The authors are thankful to Professor Sagar Mitra, Department of Energy Science and Engineering, Indian Institute of Technology, for kindly permitting use of EDX facility. The authors are also thankful to SAIF, IIT, Mumbai, for recording the TEM images of sample. One of the authors Atul B. Lavand is grateful to UGC, New Delhi, for providing BSR fellowship.

References

[1] H. Tong, S. Ouyang, Y. Bi, N. Umezawa, M. Oshikiri, and J. Ye, "Nano-photocatalytic materials: possibilities and challenges," *Advanced Materials*, vol. 24, no. 2, pp. 229–251, 2012.

[2] S. S. Shinde, C. H. Bhosale, and K. Y. Rajpure, "Kinetic analysis of heterogeneous photocatalysis: role of hydroxyl radicals," *Catalysis Reviews: Science and Engineering*, vol. 55, no. 1, pp. 79–133, 2013.

[3] C. Tian, Q. Zhang, A. Wu et al., "Cost-effective large-scale synthesis of ZnO photocatalyst with excellent performance for dye photodegradation," *Chemical Communications*, vol. 48, no. 23, pp. 2858–2860, 2012.

[4] R. Asahi, T. Morikawa, T. Ohwaki, K. Aoki, and Y. Taga, "Visible-light photocatalysis in nitrogen-doped titanium oxides," *Science*, vol. 293, no. 5528, pp. 269–271, 2001.

[5] M. Pelaez, N. T. Nolan, S. C. Pillai et al., "A review on the visible light active titanium dioxide photocatalysts for environmental applications," *Applied Catalysis B: Environmental*, vol. 125, pp. 331–349, 2012.

[6] A. B. Djurišić, Y. H. Leung, and A. M. C. Ng, "Strategies for improving the efficiency of semiconductor metal oxide photocatalysis," *Materials Horizons*, vol. 1, no. 4, pp. 400–410, 2014.

[7] U. Diebold, "The surface science of titanium dioxide," *Surface Science Reports*, vol. 48, no. 5–8, pp. 53–229, 2003.

[8] Y. Wang, Y. Huang, W. Ho, L. Zhang, Z. Zou, and S. Lee, "Biomolecule-controlled hydrothermal synthesis of C-N-S-tridoped TiO_2 nanocrystalline photocatalysts for NO removal under simulated solar light irradiation," *Journal of Hazardous Materials*, vol. 169, no. 1–3, pp. 77–87, 2009.

[9] C. Su, C.-M. Tseng, L.-F. Chen, B.-H. You, B.-C. Hsu, and S.-S. Chen, "Sol-hydrothermal preparation and photocatalysis of

titanium dioxide," *Thin Solid Films*, vol. 498, no. 1-2, pp. 259–265, 2006.

[10] T. Luttrell, S. Halpegamage, J. Tao, A. Kramer, E. Sutter, and M. Batzill, "Why is anatase a better photocatalyst than rutile?—Model studies on epitaxial TiO_2 films," *Scientific Reports*, vol. 4, article 4043, 2014.

[11] M. Liu, J. Zheng, Q. Liu et al., "The preparation, load and photocatalytic performance of N-doped and CdS-coupled TiO_2," *RSC Advances*, vol. 3, no. 24, pp. 9483–9489, 2013.

[12] G. Li, L. Wu, F. Li, P. Xu, D. Zhang, and H. Li, "Photoelectrocatalytic degradation of organic pollutants via a CdS quantum dots enhanced TiO_2 nanotube array electrode under visible light irradiation," *Nanoscale*, vol. 5, no. 5, pp. 2118–2125, 2013.

[13] S. Dutta, R. Sahoo, C. Ray et al., "Biomolecule-mediated CdS-TiO_2-reduced graphene oxide ternary nanocomposites for efficient visible light-driven photocatalysis," *Dalton Transactions*, vol. 44, no. 1, pp. 193–201, 2015.

[14] T. Lv, L. Pan, X. Liu et al., "One-step synthesis of CdS-TiO2-chemically reduced graphene oxide composites via microwave-assisted reaction for visible-light photocatalytic degradation of methyl orange," *Catalysis Science and Technology*, vol. 2, no. 4, pp. 754–758, 2012.

[15] N. Zhang, Y. Zhang, X. Pan, M.-Q. Yang, and Y.-J. Xu, "Constructing ternary CdS-graphene-TiO_2 hybrids on the flatland of graphene oxide with enhanced visible-light photoactivity for selective transformation," *The Journal of Physical Chemistry C*, vol. 116, no. 34, pp. 18023–18031, 2012.

[16] S. Prabhu, T. Viswanathan, K. Jothivenkatachalam, and K. Jeganathan, "Visible light photocatalytic activity of CeO2-ZnO-TiO_2 composites for the degradation of rhodamine B," *Indian Journal of Materials Science*, vol. 2014, Article ID 536123, 10 pages, 2014.

[17] A. B. Lavand and Y. S. Malghe, "Synthesis, characterization, and visible light photocatalytic activity of nanosized carbon doped zinc oxide," *International Journal of Photochemistry*, vol. 2015, Article ID 790153, 9 pages, 2015.

[18] J. Zhuang, Q. Tian, H. Zhou, Q. Liu, P. Liu, and H. Zhong, "Hierarchical porous TiO_2@C hollow microspheres: one-pot synthesis and enhanced visible-light photocatalysis," *Journal of Materials Chemistry*, vol. 22, no. 14, pp. 7036–7042, 2012.

[19] A. B. Lavand and Y. S. Malghe, "Nano sized C-doped TiO_2 as a visible-light photocatalyst for the degradation of 2,4,6-trichlorophenol," *Advanced Materials Letters*, vol. 6, no. 8, pp. 695–700, 2015.

[20] K. Lv, H. Zuo, J. Sun et al., "(Bi, C and N) codoped TiO_2 nanoparticles," *Journal of Hazardous Materials*, vol. 161, no. 1, pp. 396–401, 2009.

[21] A. E. Jiménez-González, J. A. Soto Urueta, and R. Suárez-Parra, "Optical and electrical characteristics of aluminum-doped ZnO thin films prepared by solgel technique," *Journal of Crystal Growth*, vol. 192, no. 3-4, pp. 430–438, 1998.

[22] K. Giribabu, R. Suresh, R. Manigandan, A. Vijayaraj, R. Prabu, and V. Narayanan, "Cadmium sulphide nanorods: synthesis, characterization and their photocatalytic activity," *Bulletin of the Korean Chemical Society*, vol. 33, no. 9, pp. 2910–2916, 2012.

[23] N. Rajeswari Yogamalar, K. Sadhanandam, A. Chandra Bose, and R. Jayavel, "Quantum confined CdS inclusion in graphene oxide for improved electrical conductivity and facile charge transfer in hetero-junction solar cell," *RSC Advances*, vol. 5, no. 22, pp. 16856–16869, 2015.

[24] G. A. Zacheis, K. A. Gray, and P. V. Kamat, "Radiolytic reduction of hexachlorobenzene in surfactant solutions: a steady-state and pulse radiolysis study," *Environmental Science and Technology*, vol. 34, no. 16, pp. 3401–3407, 2000.

[25] P. A. Sant and P. V. Kamat, "Interparticle electron transfer between size-quantized Cds and TiO_2 semiconductor nanoclustersy," *Physical Chemistry Chemical Physics*, vol. 4, no. 2, pp. 198–203, 2002.